Interdiffusion at Interfaces of Polymers with Similar Physical Properties

Woon Chun Kim, Chang Jun Lee, Hoon Goo Sim, and Hyungsuk Pak*

Department of Chemistry, Seoul National University, Seoul 151-742, Korea
Received February 18, 2000

Interdiffusion process at interfaces of chemically identical polymers (e.g., deuterated-nondeuterated pairs) with different molecular weights or polymers with similar physical properties, is studied here by varying the diffusion time. Considering the vacancy flux (J_v) and adopting the Cahn-Hilliard interfacial energy in describing this system, we can see that the variation of the interfacial composition profile with time is asymmetric and the interface moves towards the polymer with the lower molecular weight as interdiffusion progresses. Furthermore, interface shift Δx, which characterizes the interdiffusion between polymers, agrees well with the behaviors of the existing experimental data. We can also obtain the interface shift factor C, which can be converted into values of D_s (self-diffusion coefficient of the smaller molecules), from the slopes of the linear fits to the data of the interface shift.

Introduction

Polymer diffusion have been studied for many years by using the various experimental techniques and the theoretical approaches in order to understand the process of the interdiffusion between polymers with different molecular weights. One of these experiments and theoretical approaches is the interdiffusion between homopolymers with isotopically differing segments or polymers with similar physical properties.[1-6] Another is the interdiffusion between couples of chemically different, but compatible, polymers.[7-10] In all the theories above-mentioned, in spite of the differences in their basic assumptions, the bulk flows occur in order to compensate for the gap between mobilities of long and short polymers. The diffusion of a long and entangled polymer chain in the melt is adequately described by the reptation model proposed by de Gennes.[11] An important prediction of this model is that the diffusion coefficient D of a chain of degree of polymerization N should decrease as N^{-2}. Such prediction has been verified by experiments in which a very dilute concentration of deuterated polyethylene chains is allowed to diffuse into undeuterated polyethylene.[12,13] The experimental evidences, however, both from concentrated homopolymers of different molecular weights[14] and from chemically different, but compatible polymers,[15] show large deviation from the N^{-2} dependence of D expected from the naive application of the reptation model. A possible reason for these deviations has been discovered by Brochard, Jouffroy, and Levinson (BJL).[16] They showed that the diffusion coefficient D of concentrated polymer solutions depends markedly on the concentration and deviates largely from N^{-2} dependence. They made the assumption, however, that the fluxes of the diffusing species are equal and opposite. The limitation of this assumption is that the interface remains symmetric as interdiffusion proceeds for symmetric boundary conditions. On the other side, Kramer and associates[2,17] showed that, for polymers with different molecular weights, the interface moves towards the polymer with the lower molecular weight as interdiffusion proceeds. Kramer *et al.*[1] and Sillescu[18] described interdiffusion in systems with a moving interface by unequal fluxes of polymers A and B, which were balanced by a net flux (bulk flow) of vacancies (holes or free volume) across the interface. The effect of bulk flow can be compared to the swelling of a high molecular weight polymer matrix by small molecules. They assumed that the chemical potential of vacancies was zero in the melt state but the flux of vacancies was finite. In this paper, we develop a dynamic model for the interdiffusion of polymer molecules with vacancy flux, by adopting the Cahn-Hilliard interfacial energy into the existing theory[1] and transforming the variables. Here we only deal with polymer systems of chemically identical or similar species.

Theory

We consider the interdiffusion, at the lattice model, between homopolymer A of degree of polymerization N_A and homopolymer B of degree of polymerization N_B. It is assumed that the vacancies are distributed at random in the lattice and occupy a small fraction of the total concentration. Therefore, the concentration of the vacancies does not contribute to the free energy of mixing. Then, the interdiffusion is performed at the temperature T of the two-phase region, where T is not far away from the critical temperature T_c. A single chain diffusing by the reptation mechanism diffuses along its tube defined the topological constraints of neighbor chains. During this diffusion, a certain length of new tube is created at one end and destroyed at the other. For a chain to diffuse like this, a certain volume of vacant space must be created and destroyed at the two ends of the diffusing chain. This creation and destruction of volume causes a net flux of vacancies (J_v). Thus, there are three fluxes (*i.e.*, J_A, J_B, and J_v) involved in the interdiffusion. If the lattice sites are conserved with negligible excess volume of mixing and no

change in the lattice size during the interdiffusion, then:

$$J_A + J_B + J_V = 0 \tag{1}$$

For this situation the Onsager relations can be written as follows:

$$J_A = -M_A \nabla(\mu_A - \mu_V) \tag{2a}$$

$$J_B = -M_B \nabla(\mu_B - \mu_V) \tag{2b}$$

$$J_V = M_A \nabla(\mu_A - \mu_V) + M_B \nabla(\mu_B - \mu_V) \tag{2c}$$

where M_A and M_B are Onsager coefficients for the A and B molecules and where the off-diagonal coefficients $M_{AB} = M_{BA}$ are assumed to be zero. These coefficients are only important in systems with electrostatic interactions.[10] Therefore, this is a good assumption since the off-diagonal coefficients can be neglected for interdiffusion in polymer pairs without ionic group.

If the molecular weight of A and B are different, there will be a chemical potential gradient $\nabla \mu_v$. We assume that the vacancy flux J_v is not zero but rather $\nabla \mu_v = 0$, *i.e.*, that the vacancy concentration is nearly at equilibrium everywhere. If the chain relaxation time is fast compared with the experimental time, then the chemical potential of vacancies is negligible. Under this assumption, the Onsager relations become:

$$J_A = -M_A \nabla \mu_A \tag{3a}$$

$$J_B = -M_B \nabla \mu_B \tag{3b}$$

$$J_V = M_A \nabla \mu_A + M_B \nabla \mu_B \tag{3c}$$

In the long chain limit where N_A and N_B are much larger than N_{eA} and N_{eB} (the entanglement degree of polymerization of the polymers A and B, respectively), the Onsager coefficients M_A and M_B may be expressed as follows:

$$M_A = \phi B_{0A} N_{eA}/N_A \tag{4a}$$

$$M_B = (1-\phi) B_{0B} N_{eB}/N_B \tag{4b}$$

where B_{0A} and B_{0B} are the curvilinear Rouse mobilities (or monomer mobility) of the A and B segments, respectively and f is the volume fraction of polymer A.

For the interdiffusion of chemically identical polymers with isotope effect ($\chi > 0$: χ is the interaction parameter between monomers of polymers A and B) or polymers with similar physical properties of different molecular weight, $M_A = \phi B_0 N_e/N_A$ and $M_B = (1-\phi) B_0 N_e/N_B$. Here we assume that the monomer mobility (B_0) is independent of ϕ since, in the system like the above, the mobility is relatively independent of composition across the interface.

The chemical potential for each component is obtained from the functional derivative of the total free energy with respect to the volume fraction of that component. Thus, the chemical potential gradient is obtained from the derivative of chemical potential with respect to the diffusion axis. The total free energy with an extension of the Flory-Huggins theory, allowing for spatial variations of ϕ, takes a following form:

$$F = \int dV \left[f(\phi(\boldsymbol{r})) + \frac{a^2}{24\phi(1-\phi)} [\nabla \phi(\boldsymbol{r})]^2 \right] \tag{5}$$

where $f(\phi)$ is the Flory-Huggins free energy density of the system and the second term accounts for the Cahn-Hilliard interfacial energy[19] associated with the spatial variation of the composition. The characteristic length a is assumed to be the same for A and B. We also assume that the polymer-vacancy interaction parameter is negligible since the concentration of vacancies is an order of magnitude lower than the polymer concentration.

The chemical potential gradients can be found from Eq. (5):

$$\nabla \mu_A = \frac{1}{\phi} \left\{ \frac{1-\phi}{N_A} + \frac{\phi}{N_B} - 2\chi\phi(1-\phi) \right\} \nabla \phi - \frac{a^2}{12\phi} \nabla^3 \phi \tag{6a}$$

$$\nabla \mu_B = \frac{-1}{1-\phi} \left\{ \frac{1-\phi}{N_A} + \frac{\phi}{N_B} - 2\chi\phi(1-\phi) \right\} \nabla \phi + \frac{a^2}{12(1-\phi)} \nabla^3 \phi \tag{6b}$$

In arriving at Eq. (6), we have neglected nonlinear terms involving $(\nabla\phi)^3$ and $(\nabla\phi)\nabla^2\phi$.[20] If the two species A and B are not too different, χ is small: in the present paper, we concern only with the case of small positive χ.

Since polymers A and B have unequal intrinsic diffusion coefficients, J_A is not equal to J_B. In the incompressible polymer system, these unequal fluxes cause swelling of a high molecular weight polymer matrix by small molecules. The swelling can be compared to the effective "bulk flow" called by Crank,[21] and it reduces or increases the net transfer of polymer segments A and B across the interface. The bulk flow means the shift of the interface between two polymer slabs of different molecular weights. As interdiffusion progresses, the shift will be toward the lower molecular weight side. The amount of swelling is related to the net flux of vacancies across the interface. Therefore, the total flux of A is given by the following relations:

$$\begin{aligned} J_A^T &= J_A + \phi J_V \\ &= -(1-\phi) M_A \nabla \mu_A + \phi M_B \nabla \mu_B \end{aligned} \tag{7}$$

Conservation of A segments leads to:

$$\frac{\partial \phi}{\partial t} = \nabla(-J_A^T) \tag{8}$$

and combining Eqs. (4) and (6) with (8) gives:

$$\frac{\partial \phi}{\partial t} = \nabla \left\{ D_A \left(1 - \phi + \frac{\phi}{R} \right) \times \langle 1 - \phi + \frac{\phi}{R} - 2N_A\chi\phi(1-\phi) \rangle \nabla\phi - \frac{K}{2} \nabla^3 \phi \right\} \tag{9}$$

where D_A ($=B_0 N_e/N_A^2$) is the self diffusion coefficient of highly entangled linear polymer A in the melt and R ($=N_B/N_A$) represents the molecular weight ratio. The interfacial parameter K ($=N_A a^2/6$) has the magnitude of the square of the radius of gyration.

We now write the Eq. (9) in dimensionless form *via* scaling the length and the time. It is assumed that the flux is one-dimensional (denoted by the x-axis) in the direction perpen-

dicular to the interface. The length is scaled by the natural length $K^{1/2}$ in the Eq. (9) and we make the conversion $x/K^{1/2} \rightarrow x$. The time is scaled with the unit $\tau = 2K/D_A$, which is on the order of the reptation time of a single chain in the melt, and we transform $t/\tau \rightarrow t$. Finally the composition variable is redefined as $\psi = 2(\phi - ½)$ so that the order parameter ψ takes values between +1 (pure A) and −1 (pure B) as the composition ϕ drops from 1 to zero. We have also made a change of notation: $N_A\chi \rightarrow \chi$, where $\chi_c = 2$ in the critical point of the symmetric case (N_A=N_B).[22] The result in terms of the rescaled variables is given by the following equation:

$$\frac{\partial \psi}{\partial t} = \frac{\partial}{\partial x}\left\{\left[\frac{1}{2} + \frac{1}{2R} + \left(\frac{1}{2R} - \frac{1}{2}\right)\psi\right] \times \left[\langle 1 + \frac{1}{R} - \chi + \left(\frac{1}{R} - 1\right)\psi + \chi\psi^2\rangle \frac{\partial \psi}{\partial x} - \frac{\partial^3 \psi}{\partial x^3}\right]\right\} \quad (10)$$

The first term accounts for the differences in molecular weights of the two polymers; the second term involving $\partial\psi/\partial x$ accounts for the free energy of mixing; and the third term involving $\partial^3\psi/\partial x^3$ accounts for the presence of an interface separating the two incompatible phases.

The above equation is solved by application of the standard Crank-Nicholson method[20] with $\Delta t = 0.01$ and $\Delta x = 0.5$. The grid points are 700, so that the total thickness is $350K^{1/2}$. We take the initial interface of the bilayer as $300\Delta x$. The boundary condition is $\partial\psi/\partial x = 0$ and $\partial^3\psi/\partial x^3 = 0$ at the outer two ends of the bilayer.

Results and Discussion

Binary polymer mixtures with similar physical properties are characterized by the upper critical solution temperature. Therefore, the two polymers are partially miscible at the temperature lower than the critical point for miscibility. We are interested in the interdiffusion near the critical point. The transport phenomena will appear non-Fickian at the biphasic region and asymmetric in the polymers with the different molecular weight. Our numerical results are presented as follows. In Figure 1, the composition profiles for χ=1.5, 1.6, 1.7, and 1.8 are plotted at t=1000τ after onset of the interdiffusion, where the molecular weight ratio R is 2 and the critical point is χ_c = 1.46 for R=2 in the following equation: $\chi_c = (1+\sqrt{R})^2/(2R)$.[22,23,24] We can clearly see the effect of temperature (or χ-value) on the interdiffusion at the constant molecular weight as shown in Figure 1. The transport phenomena in the bilayer were found to depend strongly on the thermodynamic conditions such as temperature, interaction parameters between polymers A and B, and molecular weights of A and B. In this paper, we deal with the dynamic effects of temperature and molecular weight on the interdiffusion driven by the thermodynamic forces. According to the reptation model,[25] the reptation or disengagement time τ_d is given by:

$$\tau_d = Nb^2/3\pi^2 D^* \quad (11)$$

where N is the degree of polymerization, b is the statistical segments length, and D^* is the self-diffusion coefficient for the center of mass.[26] As the D^* is proportional to the temperature, the τ_d is inversely proportional to the temperature. Moreover, one can calculate that τ_d depends on molecular weight by an exponent of 3 by using the N^{-2} dependence of the diffusion coefficient. Therefore, at the higher temperature, the reptation time of the polymers in the entangled polymer melt is shorter and the polymers will move faster. Thus, polymers will interdiffuse better into the other polymer sheet at the higher temperature (*i.e.*, at the lower χ-value which is inversely proportional to the temperature). As shown in Figure 1, the interdiffusion speeds at four different temperatures below the critical temperature T_c, agree well with our prediction. However, the relative speed of the interdiffusion of the polymers A and B at each temperature is different due to the effect of the molecular weights. The ratio of the molecular weights for shorter molecules A, is 2 in Figure 1. The assumption is that the polymers move via reptation into vacancies that are due to thermal fluctuations continuously created and destroyed. According to the higher mobility of smaller molecules compared to the larger ones, polymers A are more likely to diffuse into vacancies. Therefore, the shorter polymers A diffuse faster and more deeply into the phase of the longer polymers B. Consequently different polymer fluxes cross the interface. This is accompanied by a flux of vacancies and leads to a shift of the position of the interface. The shift will be toward the lower molecular weight side in order to compensate for the net flux. One might compare this process to the swelling of polymers. The amount of the swelling is related to the net flux of vacancies across the interface. The vacancy flux will be detectable by marker movement in the experiments. We define the interface position at $\psi = 0$ in Figure 1 as the ref 7 did, in order to compare with experimental data. The interface shift Δx is defined as the distance from the position of the interface at t = 0τ. Figure 2 shows plots of Δx versus $t^{1/2}$ for χ = 1.5, 1.6, 1.7, and 1.8 with R = 2. The solid lines are the linear least square fits to the data. The interface shift increases linearly with $t^{1/2}$ at all diffusion temperatures. However, the slopes of

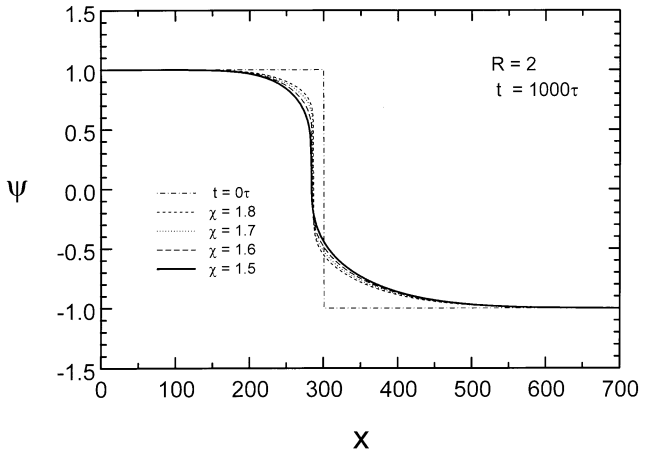

Figure 1. Composition profile of the lower molecular weight polymer A for χ=1.5, 1.6, 1.7, and 1.8 at t=1000τ and R (=N_B/N_A) =2. χ_c = 1.46 for R=2. The time is expressed in units of τ (=$2K/D_A$) and length in units of $0.5K^{1/2}$.

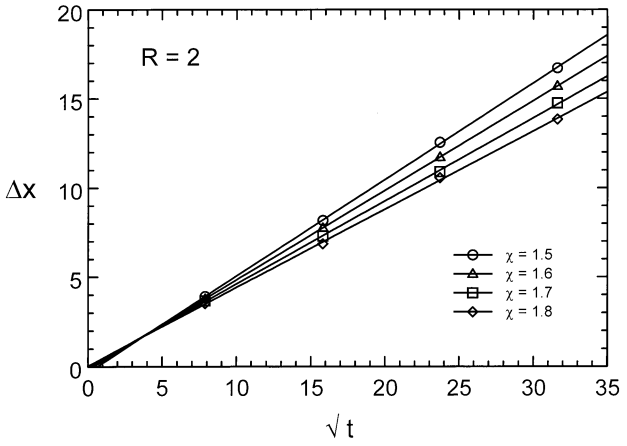

Figure 2. Interface shift versus square root of diffusion time for χ =1.5, 1.6, 1.7, and 1.8 at R=2. The units are the same as in Figure 1.

the straight lines fitted to the data are different. The interface shift (or bulk flow) increases with temperature owing to the growing difference of the intrinsic diffusion coefficients of polymers A and B. The interface behaviors in Figure 2 agree well with the experimental data.[6,7]

The following expression for the displacement of the interface is given by Green *et al.*[2]:

$$\Delta x' = C(D_s t')^{1/2} \tag{12}$$

where $\Delta x'$ is the shift of the interface, C is a constant and D_s is the diffusion constant of the smaller molecules. Therefore, the interface shift should be proportional to $t'^{1/2}$ and the slope of a plot of $\Delta x'$ *vs.* $t'^{1/2}$ should give $C(D_s)^{1/2}$. In our paper, the length was scaled by $K^{1/2}$ and the time was also scaled with the unit $2K/D_A$. The Eq. (12) using our scaled variables is converted as follows:

$$\Delta x = C\sqrt{2}t^{1/2} \tag{13}$$

From the slopes of the linear fits in Figure 2, C is determined as a function of c using the Eq. (13) and the results are displayed in Figure 3. Measurements of the interface shift in the experiments with R=2 can be converted using Figure 3 into values of D_s for the temperature (or χ-value) near the critical

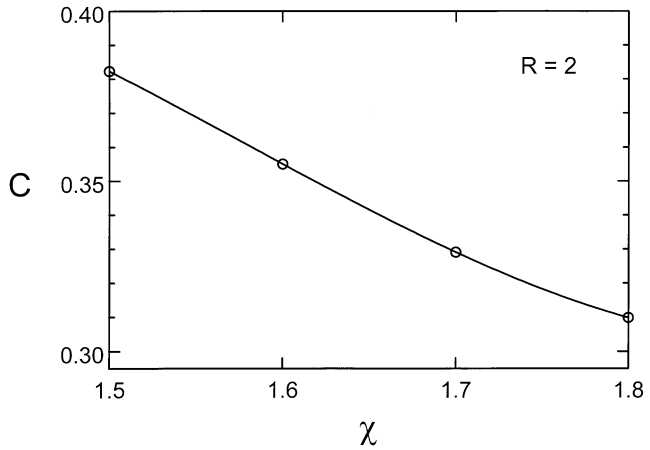

Figure 3. Computed interface shift factor C in Eq. (13) against the χ-parameter for R=2.

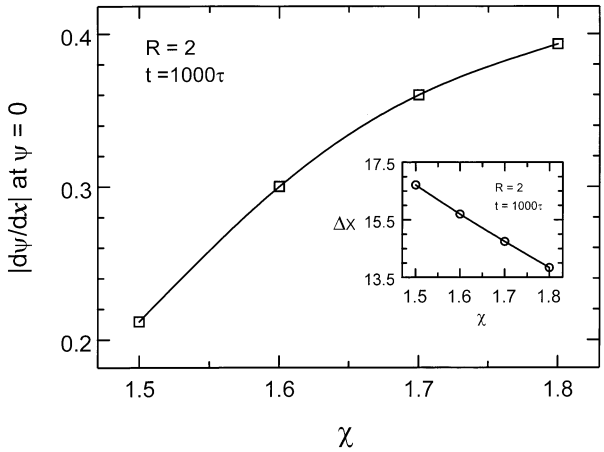

Figure 4. Absolute value of the slope at the interface and interface shift (inset) against the χ-parameter for R=2 and t=1000τ.

point. In Figure 1, the slope of the interface is different at the different temperature. Thus, our results show that the interdiffusion behavior is more asymmetric and the slope is steeper at the lower temperature. Figure 4 shows absolute values of the slopes at the interface ($\psi = 0$) of Figure 1. In Figure 4, we allow the system to evolve 10^5 time steps (=1000τ). A reason for the difference of slope with temperature is that the system at the lower temperature lies more closely to the incompatible two-phase region and the polymers become less miscible. Therefore, the interface reveals more distinct boundary between two polymers at the lower temperature. We can see the degree of the distinct boundary by the slope of the interface. Figure 5 shows the mass transport across the initial interface according to the temperature and diffusion time. The mass transport is calculated as follows:

$$\text{Mass transport} = \int_{300\Delta x}^{700\Delta x} dx[1 + \psi(x,t)] \tag{14}$$

The variations of the mass transport reveal linear relation to the χ-value regardless of the diffusion time. These behaviors are similar to the linear relation between interface shift and χ-value as shown in inset of Figure 4. Afterwards, we

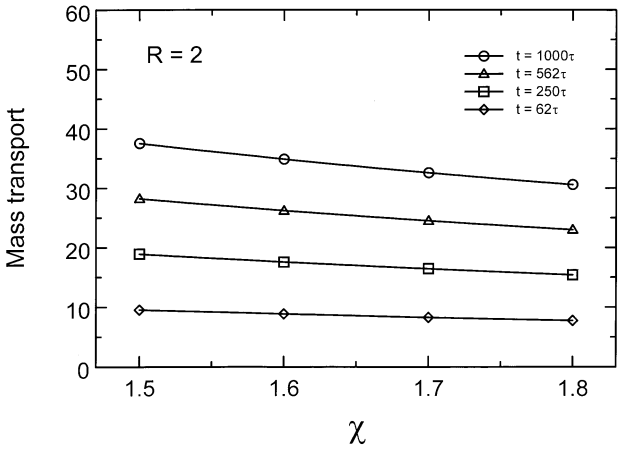

Figure 5. Mass transport calculated from the Eq. (14) *vs.* the χ-parameter for R=2 at four consecutive time t = 62τ, 250τ, 562τ, and 1000τ.

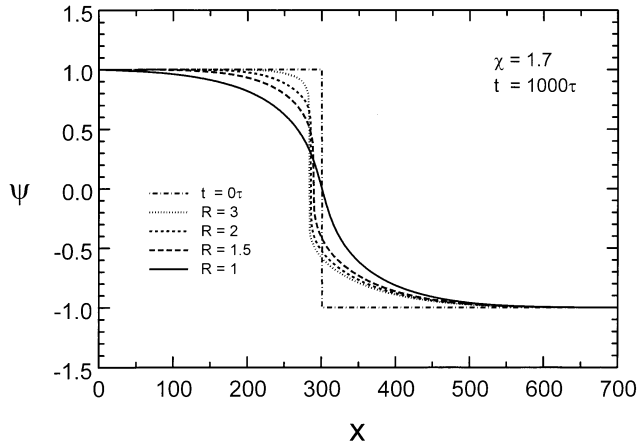

Figure 6. Composition profile of the lower molecular weight polymer A for several molecular weight ratios (R=1, 1.5, 2, and 3) at t=1000τ and χ=1.7. The units are the same as in Figure 1.

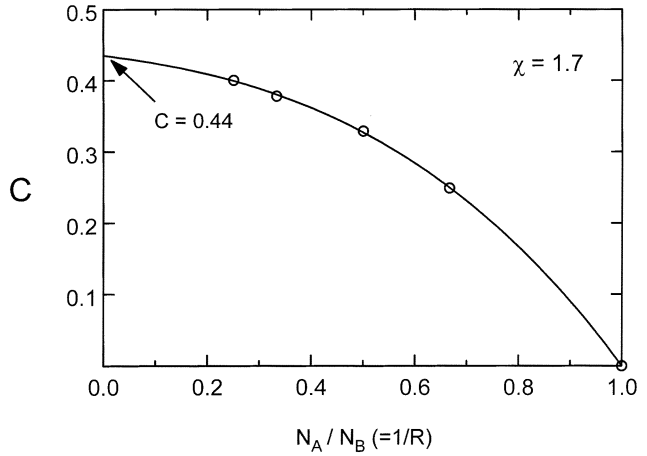

Figure 8. Computed interface shift factor C in Eq. (13) against the molecular weight ratio of polymer A to polymer B.

will compare the dynamic effects of temperature on the slope of interface, interface shift, and mass transport with the dynamic effects of the molecular weight.

Now, using our model, we will discuss the effects of molecular weight on the interdiffusion under the constant temperature. The composition profiles of the lower weight polymer A for R = 1, 1.5, 2, and 3 are shown in Figure 6. The χ-value is 1.7 and the diffusion time is 1000τ for all the molecular weight ratios. The interdiffusion in Figure 6 is symmetric[20] for R=1. As R becomes more than 1, the curves approach an asymptotic shape. These are the reason the intrinsic diffusion coefficient of the chain decreases as N^{-2}. Consequently, the difference of the polymer fluxes A and B across the initial interface becomes greater as R grows more than 1. The speed of the interdiffusion, however, reveals opposite result. Namely, the interdiffusion speed is inversely proportional to the molecular weight ratio R in Figure 6. The critical point is χ_c =1.65, 1.46, and 1.24 for R=1.5, 2, and 3, respectively.[22,23,24] Therefore, the constant χ-value of 1.7 puts the system more deeply into the two-phase region and makes the two polymers more incompatible, for the larger R. The interdiffusion behaviors in Figure 6 agree well with the simulation data.[2]

The interface shift versus $t^{1/2}$ for the various molecular weight ratios at χ=1.7 is plotted in Figure 7. The solid lines are the best straight fits to the data. In the symmetric case (R=1), there is no interface shift owing to the same fluxes of polymers A and B. However, the interface shift increases in proportion to the molecular weight ratio for R > 1. Since the lower molecular weight chains A diffuse faster than the high molecular weight chains B, the interface shifts move to the low molecular weight side of the diffusion couple at a rate, which reflects the diffusion coefficient of the faster diffusing (the low molecular weight) species A.[1] Our results in Figure 7 agree well with the behaviors of the experimental data.[2,5] By the way, the increment of the interface shift is reduced with the R-value as shown in inset of Figure 9. Those trends relate to the constant C. The slope of the each line in Figure 7 yields the constant C in Eq. (13). From the Eq. (13), C is determined as a function of N_A/N_B (=1/R) and the results are displayed in Figure 8. The value of C approaches a limiting value of 0.44 as $N_A << N_B$, which is similar to 0.48 of ref 2. Using Figure 8, measurements of interface shift with 1/R in the experiment can give values of D_s for any different N_A and

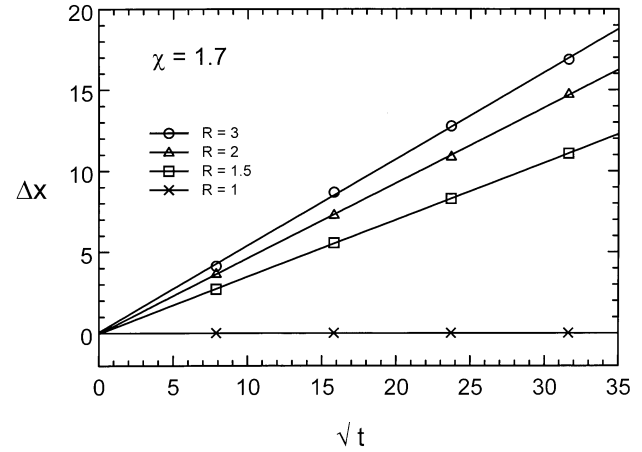

Figure 7. Interface shift versus square root of diffusion time for R = 1, 1.5, 2, and 3 at χ=1.7. The units are the same as in Figure 1.

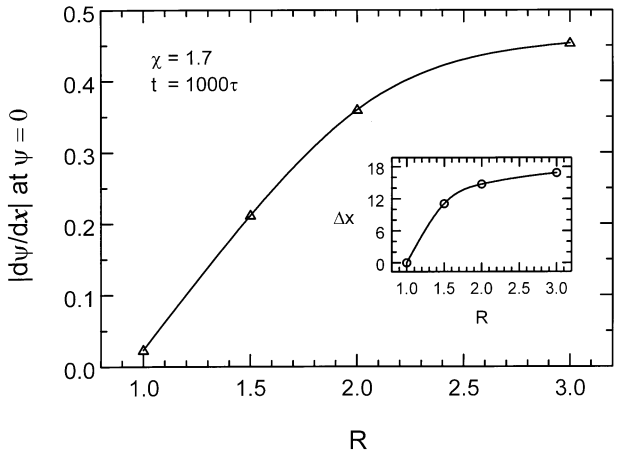

Figure 9. Absolute value of the slope at the interface and interface shift (inset) against the molecular weight ratio R at t=1000τ and χ =1.7.

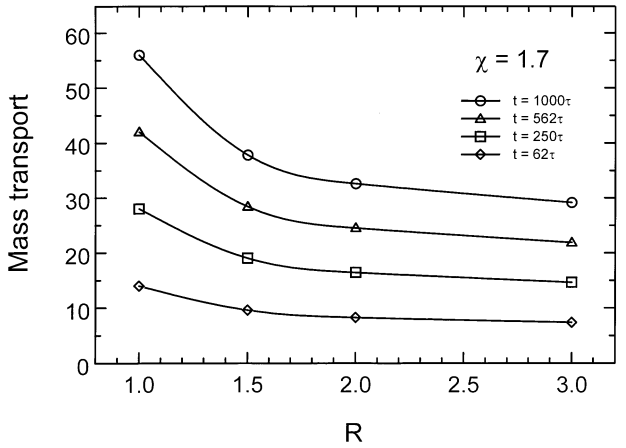

Figure 10. Mass transport calculated from the Eq. (14) against the molecular weight ratio R for χ=1.7 at four consecutive time t = 62τ, 250τ, 562τ, and 1000τ.

N_B at χ=1.7. Figure 9 shows, in the time τ=1000τ, the absolute values of the slopes versus R at the interface of Figure 6. In the higher R, the slope is steeper but decreases in the rate of increase. The interface shift is also proportional to the molecular weight ratio but reduce in the increasing rate as shown in inset of Figure 9. For the constant χ-value (χ=1.7), the lager R, the deeper the system lies into the two-phase region. Therefore, the interface reveals the narrower interface width and the slope is slanter, for the larger R. Furthermore, since the short polymers A of the larger R-value diffuse faster compared with ones of the smaller R-value, the interface shift increases with R to compensate for the difference of the materials crossing the interface. Comparing Figure 9 for the constant χ-value with the Figure 4 for the constant R-value, we can see the following results. Both the slope of the interface and the interface shift in Figure 9 increase with R-value, while in Figure 4 the slope of the interface increase but the interface shift decrease with χ-value. Figure 10 shows the mass transport defined as Eq. (14) at χ=1.7.

The mass transports across the initial interface are inversely proportional to the R-value. Finally, we are able to conclude that mass transports are more affected by the R-value ($1 < R < 2$) than by the χ-value comparing Figure 10 with Figure 5.

Conclusions

Introducing the Cahn-Hilliard interfacial energy and vacancy flux into the existing model and simplifying the diffusion equation by rescaling the variables, we can derive the dynamical interdiffusion equation applied to the polymer pair with similar physical properties, to predict the composition profile at the interface below the critical temperature. Using our model, we can see the dynamic effects of the temperature and the molecular weight ratio on the interdiffusion. The composition profiles are asymmetric for the different molecular weight as we anticipated and agree well with the behaviors of the simulation data. The interface shifts calculated from the composition profiles show the exact linear dependence on $t^{1/2}$, which agree well with the experimental results. Furthermore, the constant C calculated from the Eq. (13) can be converted using Figure 3 and Figure 8 into the values of D_s for the limited different temperature and molecular weight ratio. Comparing Figure 5 with Figure 10, though our results are confined to the certain temperature and molecular weight ratio, we can see that the molecular weight ratio has larger effects on the mass transport of the interdiffusion than the temperature, near the critical point. Therefore, these results suggest that we can control, under the limited conditions, the mass transport between the polymer pairs with similar physical property more efficiently by varying the molecular weight ratio than by varying the temperature, near the critical point.

Acknowledgment. Financial support (in part) from the Brain Korea 21 program is gratefully acknowledged.

References

1. Kramer, E. J.; Green, P. F.; Palmstrom, C. J. *Polymer* **1984**, *25*, 473.
2. Green, P. F.; Palmstrom, C. J.; Mayer, J. W.; Kramer, E. J. *Macromolecules* **1985**, *18*, 501.
3. Chaturvedi, U. K.; Steiner, U.; Zak, O.; Krausch, G.; Klein, J. *Phys. Rev. Lett.* **1989**, *63*, 616.
4. Steiner, U.; Krausch, G.; Schatz, G.; Klein, J. *Phys. Rev. Lett.* **1990**, *64*, 1119.
5. Reiter, G.; Huttenbach, S.; Foster, M.; Stamm, M. *Macromolecules* **1991**, *24*, 1179.
6. Shearmur, T. E.; Clough, A. S.; Drew, D. W.; van der Grinten, M. G. D.; Jones, R. A. L. *Polymer* **1998**, *39*, 2155.
7. Composto, R. J.; Kramer, E. J. *J. Mater. Sci.* **1991**, *26*, 2815.
8. Sauer, B. B.; Walsh, D. J. *Macromolecules* **1991**, *24*, 5948.
9. Jabbari, E.; Peppas, N. A. *Macromolecules* **1993**, *26*, 2175.
10. Jabbari, E.; Peppas, N. A. *Polymer* **1995**, *36*, 575.
11. de Gennes, P. G. *J. Chem. Phys.* **1971**, *55*, 572.
12. Klein, J. *Nature* **1978**, *271*, 143.
13. Klein, J. *Macromolecules* **1981**, *14*, 460.
14. Kumagai, Y.; Watanabe, H.; Miyasaka, K.; Hata, T. *J. Chem. Eng. Japan* **1979**, *12*, 1.
15. Gilmore, P. T.; Falabella, R.; Lawrence, R. L. *Macromolecules* **1980**, *13*, 880.
16. Brochard, F.; Jouffroy, J.; Levinson, P. *Macromolecules* **1983**, *16*, 1638.
17. Tead, S. F.; Kramer, E. J. *Macromolecules* **1988**, *21*, 1513.
18. Sillescu, H. *Makromol. Chem., Rapid Commun.* **1987**, *8*, 393.
19. Cahn, J. W.; Hilliard, J. E. *J. Chem. Phys.* **1958**, *28*, 258.
20. Wang, S.-Q.; Shi, Q. *Macromolecules* **1993**, *26*, 1091.
21. Crank, J. *The Mathematics of Diffusion*; Oxford University Press: Oxford, 1975.
22. de Gennes, P. G. *Scaling Concepts in Polymer Physics*; Cornell Univ. Press: Ithaca, New York, 1979.
23. Kim, W. C.; Pak, H. *Bull. Korean Chem. Soc.* **1999**, *20*, 1323.
24. Kim, W. C.; Pak, H. *Bull. Korean Chem. Soc.* **1999**, *20*, 1479.
25. de Gennes, P. G. *J. Chem. Phys.* **1971**, *55*, 572.
26. Doi, M.; Edwards, S. F. *The Theory of Polymer Dynamics*; Oxford University Press: Oxford, 1986.